A Two-zone fire growth and smoke movement model for multi-compartment buildings

Fu, Z.; Hadjisophocleous, G. V.

Publisher's version / Version de l'éditeur:
https://doi.org/10.1016/S0379-7112(99)00045-4
Fire Safety Journal, 34, April 3, pp. 1-30, 2000-04-01

National Research Council Canada
Conseil national de recherches Canada

NRC · CNRC

A Two-zone fire growth and smoke movement model for multi-compartment buildings

Fu, Z.; Hadjisophocleous, G. V.

NRCC-41111

A version of this paper is published in / Une version de ce document se trouve dans :
Fire Safety Journal. V. 34, no. 3, April 2000, pp. 257-285

www.nrc.ca/irc/ircpubs

A Two-Zone Fire Growth and Smoke Movement Model for Multi-Compartment Buildings

Zhuman Fu and George Hadjisophocleous

Fire Risk Management Program, Institute for Research in Construction, National Research Council of Canada, Ottawa K1A 0R6, Canada

ABSTRACT

A fire growth and smoke movement model for a multi-compartment building has been developed at the National Research Council of Canada. This development is primarily intended to help evaluate the risk from fires in buildings. This paper presents the related physical models, numerical methods, and some verification examples. The 2-zone ordinary differential equations (ODEs) are derived for the compartments with fire or smoke. The four independent variables for one compartment are selected as pressure, enthalpy of upper layer, and mass of upper and lower layers. The implemented fire sub-models are introduced, including combustion, fluid flow and heat transfer models. For each compartment without smoke or fire, a non-linear algebraic equation based on mass conservation is used instead of the ODEs. The numerical solution of the governing equations is obtained using a room by room iteration method. In this algorithm, an existing ODE solver, LSODA, has been modified and used to solve the stiff ODEs, and the Steffensen Acceleration Method is used to solve the algebraic equations. Experimental data for single and two-compartment fire tests are compared to the predictions of the model. The comparison shows favourable results, especially for the upper layer gas temperature, interface height, and vent flow rate.

NOMENCLATURE

A	Area (m^2)
A_{CV}	Area of the ceiling vent (m^2)
A_{DV}	Area of part of a door/window type vent (m^2)
A_{int}	Area of interface (m^2)
A_w	Surface area of a wall, ceiling or floor (m^2)
C	Specific heat (J/kgK)
C_{CV}	Coefficient of ceiling vent flow
C_{DV}	Coefficient of door/window type vent flow
C_{LOL}	Lower oxygen limiting coefficient
C_P, C_V	Specific heat at constant pressure or volume (J/kgK)
C_{soot}	Volume fraction of soot in smoke layer
E	Internal energy (J)
F_{kj}	Configuration factor from surface k to surface j for radiation
FO_S	Stoichiometric fuel to oxygen ratio

FO_P	Fuel to oxygen ratio in fire plume
H	Enthalpy (J)
$\dot{H}_{si}$	Rate of net enthalpy gain of layer i by mass flow across its boundary (W)
h	Convection heat transfer coefficient (W/m^2K)
h_{IC}, h_{OC}	Convection heat transfer coefficients of the inside and outside surface of a wall, ceiling or floor (W/m^2K)
$(\Delta H)_F$	Heat of combustion per unit kilogram fuel (J/kg)
$(\Delta H)_O$	Heat of combustion per unit kilogram oxygen (J/kg)
K	Conductivity (W/mK)
L	Thickness of a wall, ceiling or floor (m)
Le	Equivalent mean beam length of gas volume for radiation (m)
m	Mass (kg)
m_{BF}	Mass of the burned fuel (kg)
m_C	Mass of carbon in fuel (kg)
m_{CO}	Mass production of CO (kg)
m_{CO_2}	Mass production of CO_2 (kg)
m_{CRP}	Mass production of carbon-related products (Soot+CO+CO_2) (kg)
$\dot{m}_e$	Mass entrainment rate (kg/s)
$\dot{m}_{Fan}$	Specified mass exhaust rate of the fan (kg/s)
m_H	Mass of hydrogen in fuel (kg)
m_{H_2O}	Mass production of water (kg)
$\dot{m}_{max}$	Maximum smoke exhaust rate from the upper layer (kg/s)
$\dot{m}_{ML}$	Mass flow rate exhausted from lower layer (kg/s)
$\dot{m}_{MU}$	Mass flow rate exhausted from upper layer (kg/s)
m_O	Mass of oxygen in fuel (kg)
m_{O_2}	Oxygen consumption from air in combustion (kg)
m_{PF}	Mass of fuel pyrolysis (kg)
$m_{PF_{min}}$	Mass production of the minimal part of fuel (kg)
m_{soot}	Mass production of soot (kg)
m_{tox1}	Mass of the first kind of toxic species of m_{PFmin} (kg)
m_{tox2}	Mass of the second kind of toxic species of m_{PFmin} (kg)
m_{tox3}	Mass of the third kind of toxic species of m_{PFmin} (kg)
m_{TUF}	Mass of the total unburned fuel (kg)
$\dot{m}_e$	Net mass flow rate entering a layer by plume entrainment (kg/s)
$\dot{m}_{e,K}$	Net mass flow rate of species K entering a layer by plume entrainment (kg/s)
$\dot{m}_{si}$	Net mass gain rate of layer i by mass flow through its boundary (kg/s)
$\dot{m}_V$	Net mass flow rate entering a layer by vent flow (kg/s)

$\dot{m}_{V,K}$	Net mass flow rate of species K entering a layer by vent flow (kg/s)
NS	Number of species
P	Pressure (Pa)
P_b	Pressure difference at the bottom position (Pa)
P_{CO_2}	Partial pressure of CO_2 (Atmosphere)
P_g	Gas pressure (Atmosphere)
P_{H_2O}	Partial pressure of water vapour (Atmosphere)
P_t	Pressure difference at the top position (Pa)
Q	Heat release rate (W)
Q_c	Convection heat release rate (W)
Q_{ceil}	Convection heat loss to ceiling surface (W)
q_{ceil}	Convection heat flux to ceiling surface (W/m^2)
Q_{conv}	Convection heat loss to a surface of a wall, ceiling or floor (W)
q_{conv}	Convection heat flux to a surface of a wall, ceiling or floor (W/m^2)
Q_F	Heat release rate directly radiated out of the fuel (W)
q_j	Net radiation heat transfer rate of surface j (W/m^2)
Q_N	Nominal heat release rate of the fuel (W)
q_{IR}	Net radiation heat flux to the inside surface of a wall, ceiling or floor (W/m^2)
q_{OR}	Net radiation heat flux to the outside surface of a wall, ceiling or floor (W/m^2)
Q_{si}	Net heat gain rate of layer i by heat transfer or combustion (W)
R	Gas constant (J/kgK)
R_C	Radius of the circular equivalent ceiling surface (m)
$\dot{S}_i$	Net energy gain rate of layer i as a source term (W)
T	Temperature (K)
t	Time (s)
T_a	Ambient temperature (K)
T_{ad}	Adiabatic ceiling jet temperature (K)
T_{ceil}	Ceiling surface temperature (K)
T_g	Gas layer temperature (K)
T_I	Interface temperature used for limiting maximum entrainment rate (K)
T_w	Temperature of the surface of a wall, ceiling or floor (K)
T(x, 0)	Initial temperature profile of a wall, ceiling or floor (K)
V	Volume (m^3)
x	Spatial coordinate in heat conduction equation (m)
Y_k	Mass fraction of species K
Y_{LOL}	Lower oxygen limiting mass fraction
Y_{O_2}	Oxygen mass fraction
Z	Height (m)
Z_e	Plume entrainment height (m)
Z_{ext}	Mechanical ventilation opening extension (m)
Z_S	Thickness of smoke layer (m)

Greek symbols

ρ	Density (kg/m^3)
γ	Ratio of specific heats
γ_{CO}	Mass ratio of CO production to carbon-related products (CO+CO_2+Soot)
γ_{Soot}	Mass ratio of soot production to carbon-related products
$\boldsymbol{\varepsilon}_{CO_2}$	Emittance of CO_2
ε_D	Emittance reduction resulting from spectral overlap
ε_g	Gas total emittance
$\boldsymbol{\varepsilon}_{H_2O}$	Emittance of water vapour
ε_j	Emissivity of surface j
ε_{soot}	Emittance of soot
σ	Stefan-Boltzmann constant (5.67×10^{-8}W/m^{2}K^4)
δ_{kj}	Kronecker function
τ_{kj}	Radiation transmittance from surface k to surface j
α_{kj}	Radiation absorptance from surface k to surface j
ϕ	Equivalence ratio
χ_C	Mass fraction of carbon in the fuel
χ_H	Mass fraction of hydrogen in the fuel
χ_{tox1}	Mass ratio of the first kind of toxic species to fuel
χ_{tox2}	Mass ratio of the second kind of toxic species to fuel
χ_O	Mass fraction of oxygen in the fuel
$\dot{\boldsymbol{\Omega}}_i$	Net mass gain rate of layer i by mass flow through its boundary (kg/s)

1. INTRODUCTION

Modelling of fire in a compartment can be achieved either using a zone modelling approach or a field modelling method. In this study, the zone modelling approach was used in which the gas within each compartment is generally divided into one, or a few, control volumes (zones), and for each zone, the physical parameters such as gas temperature and species concentrations are assumed to be spatially uniform. Then, from the mass and energy conservation principle as well as the ideal gas law, a set of ordinary differential equations (ODEs) are derived. In this type of model, the physical details of the gas within a zone are not considered, while mass and energy transport between zones is calculated by modelling the relevant fire sub-processes: combustion, fluid flow and heat transfer.[1-6]

Zone models may be grouped into two types based on the number of the control volumes (zones) in each compartment: one-zone models and two-zone models. One-zone models are widely used in the analysis of post-flashover fires, as well as smoke movement in the compartments remote from the fire room (network models). Two-zone models divide the gas in a compartment into two distinct zones: an upper, higher temperature zone and a lower, lower-temperature zone. These zones are a result of buoyancy-induced thermal stratification. Two-zone models can be used to analyze pre-flashover fires, and some

models of this type have been developed.[7-9] A comprehensive review of existing fire models can be found in Friedman.[7]

The one-zone modelling concept dates back to the work of Kawagoe et al,[10] who developed a single-zone approach for analyzing a post-flashover fire. This approach was the basis of the development of a series of single-zone post-flashover fire models.[11] The application of the two-zone method was pioneered by Thomas et al,[12] who constructed a steady state, two-layer model for calculating the flow of smoke through roof vents.[11, 13] Before the mid-1970s, however, fire modelling research was focussed on post flashover fires; i.e., fully developed fires, using the one-zone method.[14]

As Quintiere has mentioned,[5] two-zone fire modelling of pre-flashover fires emerged in the mid-1970s with the publication of a basis for the zone model approach by Fowkes[15] in his work with Emmons. Almost simultaneously, several zone computer models were produced by Quintiere,[16] Pape and Waterman[17] and Mitler[18] working with Emmons. In the late 1970s, the first Harvard model and code was completed by Emmons and Mitler,[18] which might be the first comprehensive room fire model for one compartment.[19] However, as mentioned by Jones and Forney,[1] the first true multi-compartment model of this type was formulated by Tanaka,[20] in which the gases through a vertical vent (door or window) are assumed to flow between adjacent layers and the flow rates are computed using the state properties of the neighbouring zones of the vent. Zone modelling work continued, especially at NIST where models such as FIRST,[21] FAST[22] and CCFM[23] were developed. Jones and Forney et al[1-3] developed the CFAST model based on FAST and CCFM, in which the conservation equations are solved in their original differential form. The governing equation set of CFAST is formulated to allow the actual physical phenomena to be couched as source terms.[1, 2] The pressure is not assumed to be in the steady state, nor the lower layer temperature to be at ambient conditions.[1]

The National Research Council of Canada (NRC) has been conducting research work on the fire risk evaluation of buildings which has resulted in a comprehensive fire risk evaluation model called FiRECAM™ (Fire Risk Evaluation and Cost Assessment Model) for residential and office buildings.[24-26] Currently, research on fire risk evaluation of industrial buildings is being undertaken to develop a model for industrial buildings called FIERAsystem (Fire Evaluation and Risk Assessment system).[27] As part of the FIERAsystem model, the model described in this paper will be used to calculate smoke movement in industrial buildings.[28] FIERAsystem and its sub-models are coded using the Visual Basic programming language.

The smoke movement model presented uses similar concepts to the ones used in other two-zone models such as CFAST, however, in a number of areas the approach followed is unique. Some of the main differences between this model and CFAST are the following:

- Two-zone ODEs are solved only for the compartments with fire or smoke. For other compartments, algebraic equations are solved. The approach followed to derive the system of ODEs is new. The selection of the four independent solution variables is new. They are pressure, enthalpy of upper layer, and mass of upper and lower layers.

- The heat release rate model, used by CFAST, is re-expressed based on the concept of the equivalence ratio ϕ, which is more flexible for further development. The combustion chemistry model can be applied to pure hydrogen combustion and also to cases where there is no CO_2 production.
- The radiation model is a two-surface model,[6, 29] and the derived equations are applicable to both the fire and non-fire compartments.
- The numerical method used is different from the method used in CFAST and other two-zone models. This new method solves the governing equations room by room. The ODE solver LSODA[30] is used to solve the stiff ODEs for the compartments with fire or smoke, while the Steffensen Acceleration Method[31] is used to solve the algebraic equations for the compartments without smoke or fire.

As the model is intended for use in industrial-type buildings where forced ventilation is usually used to extract smoke from a compartment, a specification-type mechanical ventilation model was developed. This model can be applied to openings flush with the ceiling or floor, as well as to openings that extend into the compartment.

2. GOVERNING ODE EQUATIONS

2.1 Derivation of the Two-Zone Ordinary Differential Equations

Following the two-zone modelling concept, each compartment is divided into two zones. For each zone, the mass, internal energy, enthalpy, density, temperature and volume are denoted as m_i, E_i, H_i, ρ_i, T_i and V_i, respectively, where i=U refers to the upper layer, and i=L refers to the lower layer. The thermodynamic pressures for the upper and lower layers, P_U and P_L are assumed to be identical and are denoted as P. Using thermodynamic relations and definitions as well as the ideal gas law, the following equations are given:

$$\rho_i = \frac{m_i}{Vi} \tag{2.1}$$

$$E_i = C_V m_i T_i \tag{2.2}$$

$$H_i = E_i + PV_i \tag{2.3}$$

$$P = \rho_i R T_i \tag{2.4}$$

$$V = V_U + V_L \tag{2.5}$$

The coefficients C_V and C_P are assumed to be constant for the gas at the upper and lower layers, and the following relation exists:

$$\gamma = C_P / C_V, \qquad R = C_P - C_V \tag{2.6}$$

where R is the gas constant. Applying Equations (2.1) to (2.5) to both the upper and lower layers in a compartment results in 9 independent algebraic equations with thirteen variables. To close the equation set, four additional independent equations are needed, which can be obtained by applying mass and energy conservation principles to each zone. The resulting equations are as follows:

Mass conservation:

$$\frac{dm_i}{dt} = \dot{m}_{si} \tag{2.7}$$

Energy conservation (First Law):[32]

$$\frac{dE_i}{dt} + P\frac{dV_i}{dt} = \dot{H}_{si} + Q_{si} \tag{2.8}$$

where $\dot{m}_{si}$ is the net mass gain rate of layer i by mass flow across the boundary,

$\dot{H}_{si}$ is the rate of the net enthalpy gain of layer i by mass flow across the boundary,

Q_{si} is the rate of net heat gain of layer i by heat transfer or combustion.

Thus, the whole equation set has been closed. To facilitate the solution, the above system of ODEs can be converted into other forms as given below.

Denote:

$$\dot{\Omega}_i = \dot{m}_{si} \tag{2.9}$$

$$\dot{S}_i = \dot{H}_{si} + Q_{si} \tag{2.10}$$

Following the approach used in CFAST, $\dot{\Omega}_i$ and $\dot{S}_i$ are considered to be source terms. Equations (2.7) and (2.8) give:

$$\frac{dm_i}{dt} = \dot{\Omega}_i \tag{2.11}$$

$$\frac{dE_i}{dt} + P\frac{dV_i}{dt} = \dot{S}_i \tag{2.12}$$

Adding the Term $V_i \frac{dP}{dt}$ to the two sides of Equation (2.12), and considering Equation (2.3), yields:

$$\frac{dH_i}{dt} = \dot{S}_i + V_i \frac{dP}{dt} \tag{2.13}$$

Adding the upper and lower layer versions of Equation (2.13), results in:

$$\frac{d(H_U + H_L)}{dt} = (\dot{S}_L + \dot{S}_U) + V \frac{dP}{dt} \tag{2.14}$$

Equations (2.1), (2.2), (2.3), (2.4) and (2.6), give:

$$H_i = \frac{C_P}{R} V_i P \tag{2.15}$$

Adding the upper and lower layer versions of Equation (2.15), and substituting into Equation (2.14), yields:

$$\frac{dP}{dt} = \frac{\gamma - 1}{V} (\dot{S}_U + \dot{S}_L) \tag{2.16}$$

In this model, P, H_U, m_U, m_L have been selected as the solution variables of the governing equation set as follows:

$$\frac{dP}{dt} = \frac{\gamma - 1}{V} (\dot{S}_U + \dot{S}_L) \tag{2.17}$$

$$\frac{dH_U}{dt} = \dot{S}_U + V_U \frac{dP}{dt} \tag{2.18}$$

$$\frac{\mathrm{dm_U}}{\mathrm{dt}} = \dot{\mathbf{\Omega}}_{\mathrm{U}} \tag{2.19}$$

$$\frac{\mathrm{dm_L}}{\mathrm{dt}} = \dot{\mathbf{\Omega}}_{\mathrm{L}} \tag{2.20}$$

The ODE equations, where the independent variables are layer internal energy, layer volume, layer density and layer temperature, can be found in Jones and Forney.[1, 33] In the literature,[1, 3, 6, 33] the two terms on the right side of Equation (2.8) were combined as one term, called enthalpy or total enthalpy. This could result in a little confusion between this term and the real thermodynamic enthalpy term. Thus, in this derivation, Equation (2.13) for thermodynamic layer enthalpy is presented as complementary to the table "Conservative Zone Modeling Differential Equations" appearing in the literature,[1, 3, 33] although H_i is directly proportional to E_i by γ in this case.

In the above governing equations, the mass and energy source terms, $\dot{\mathbf{\Omega}}_i$ and $\dot{S}_i$, are obtained by modelling the relevant fire sub-processes, combustion, fluid flow and heat transfer. Sections 3, 4 and 5 will present the details of modelling these processes.

2.2 The Algebraic Governing Equations for Constant Temperature Compartments

For compartments with fire or smoke, the two-zone ODEs derived in the above section need to be solved. However, for compartments without smoke or fire (fire or smoke has not propagated here), generally only a non-linear algebraic equation of pressure based on mass conservation needs to be solved. In this code, a mechanism is implemented to judge whether it is necessary to solve the differential equations based on the estimation of the gas temperature differences between the compartment being solved and its directly connected compartments. If one of the temperature differences is considerably large, then the ODE solver is called. Otherwise, a non-linear algebraic equation of pressure based on the constant mass assumption is solved as follows:[34]

$$\sum_{K=1}^{NV} \dot{m}_K(P_0, P_K) = 0 \tag{2.21}$$

where $\dot{m}_K$ is the mass flow rate through vent K, which is connected to the compartment being solved; $\dot{m}_K$ is a function of the pressure difference between the two sides of the vent, P_0 and P_K; P_0 is the pressure of the compartment being solved, and P_K is the pressure of the compartment connected to the solved compartment through vent K; NV is the number of vents connected to the compartment being solved.

In this model, Bernoulli's equation is used to calculate the mass flow rate, $\dot{m}_K$. Equation (2.21) is numerically solved using Steffensen Acceleration Method.[31]

3. COMBUSTION

3.1 Heat Release Rate

The heat release rate in unconstrained combustion can be obtained by:

$$Q_N = \dot{m}_{PF}(\Delta H)_F \tag{3.1}$$

where $(\Delta H)_F$ is the effective heat of combustion per unit kilogram fuel in open air, and $\dot{m}_{PF}$ is the mass pyrolysis rate. Following the oxygen consumption principle, the oxygen consumption rate can be obtained using:[35, 36]

$$\dot{m}_{O_2} = \frac{Q_N}{(\Delta H)_O} \tag{3.2}$$

where $(\Delta H)_O$ is the heat of combustion per unit kilogram oxygen. For complex fuels, it could be taken as 13.2 MJ/kg,[37] while, for simple chemical formula fuels, it could be obtained from the value of heat of combustion per unit kilogram fuel.

The stoichiometric fuel to oxygen ratio, FO_S, is:

$$FO_S = \frac{(\Delta H)_O}{(\Delta H)_F} \tag{3.3}$$

The actual fuel to oxygen ratio in the fire plume is:

$$FO_P = \frac{\dot{m}_{PF}}{\dot{m}_e Y_{O_2}} \tag{3.4}$$

where $\dot{m}_e$ is the mass entrainment rate of the plume, and thus the equivalence ratio, ϕ, is:

$$\phi = \frac{FO_P}{FO_S} = \frac{(\Delta H)_F \dot{m}_{PF}}{(\Delta H)_O \dot{m}_e Y_{O_2}} \tag{3.5}$$

The actual heat release rate is considered to be related to ϕ as follows:

$$Q = f(\phi)\dot{m}_{PF}(\Delta H)_F \tag{3.6}$$

In this model, $f(\phi)$ is obtained using the following simple relation used by CFAST:

$$f(\phi) = \frac{1}{\max(\phi,1)} \tag{3.7}$$

The fuel rich flammability is given by a limiting oxygen mass or volume fraction. In order to make the calculation smooth near the fuel rich limit, following CFAST, a limiting coefficient C_{LOL} is introduced:[3]

$$C_{LOL} = \frac{\mathrm{Tanh}(800(Y_{O_2} - Y_{LOL}) - 4) + 1}{2} \tag{3.8}$$

and

$$Q = \frac{Q_N C_{LOL}}{\max(\phi,1)} \tag{3.9}$$

where Tanh(x) is the hyperbolic tangent function of x, and Y_{LOL} is the limiting oxygen mass fraction.[38]

The mass of total burnt fuel and consumed oxygen is given as:

$$\dot{m}_{BF} = \frac{Q}{(\Delta H)_F} \tag{3.10}$$

$$\dot{m}_{O_2} = \frac{Q}{(\Delta H)_O} \tag{3.11}$$

This model is similar to CFAST's but re-expressed based on the concept of the global equivalence ratio ϕ.

3.2 Combustion Chemistry

In this model, combustion chemistry is considered as follows:

$$m_{PF}[m_{PF\min} + m_{CHO}] + m_{O_2} \rightarrow m_{crp}[m_{CO_2} + m_{CO} + m_{Soot}] + m_{H_2O} + m_{PF\min} + m_{TUF} \tag{3.12}$$

m_{PF} is the mass of fuel pyrolysis, composed of two parts, $m_{PF\min}$ and m_{CHO}.

$m_{PF\min}$ is assumed to be composed of some harmful species, such as HCl and HCN, whose mass is much less than m_{PF} and will not further be involved in the combustion process. Thus $m_{PF\min}$ from m_{PF} on the left side of Equation (3.12) directly goes into its right side. In this model, $m_{PF\min}$ can be composed of as many as three kinds of toxic species: m_{tox1}, m_{tox2} and m_{tox3}.

m_{CHO} is the mass of the fuel pyrolysis excluding $m_{PF\min}$; it is assumed to be composed of carbon, hydrogen and oxygen.

The mass production of CO_2, CO and soot are combined into one new term m_{CRP}, carbon-related products, and soot is assumed to be carbon only.

m_{TUF} is the mass production of total unburned fuel, which is assumed to have the same element composition as m_{CHO}.

The following presents the calculation formulas of the combustion chemistry.

The composition of the pyrolyzed fuel is defined by the following five mass ratios, which are input from the user of the model.

$$\chi_C = m_C / m_{PF} \tag{3.13}$$

$$\chi_H = m_H / m_{PF} \tag{3.14}$$

$$\chi_O = m_O / m_{PF} \tag{3.15}$$

$$\chi_{\text{tox1}} = \text{m}_{\text{tox1}} / \text{m}_{\text{PF}} \tag{3.16}$$

$$\chi_{\text{tox2}} = \text{m}_{\text{tox2}} / \text{m}_{\text{PF}} \tag{3.17}$$

where χ_{C}, χ_{H}, χ_{O}, χ_{tox1} and χ_{tox2} are mass fractions of carbon, hydrogen, oxygen, and the first and second kinds of toxic species in the pyrolyzed fuel, respectively.

Based on the above five mass ratios, the toxic species production is then computed using:

$$m_{PF\,\text{min}} = [1 - (\chi_C + \chi_H + \chi_O)]m_{PF} \tag{3.18}$$

$$\text{m}_{\text{tox1}} = \chi_{\text{tox1}} \text{m}_{\text{PF}} \tag{3.19}$$

$$\text{m}_{\text{tox2}} = \chi_{\text{tox2}} \text{m}_{\text{PF}} \tag{3.20}$$

$$\text{m}_{\text{tox3}} = \text{m}_{\text{PF min}} - (\text{m}_{\text{tox1}} + \text{m}_{\text{tox2}}) \tag{3.21}$$

The mass ratios of the production of soot and carbon monoxide to the carbon related products, γ_{CO} and γ_{soot}, are also defined by the user:

$$\gamma_{CO} = m_{CO} / m_{CRP} \tag{3.22}$$

$$\gamma_{\text{soot}} = \text{m}_{\text{soot}} / \text{m}_{\text{CRP}} \tag{3.23}$$

Then the production of the carbon-related products of combustion can be obtained from:

$$\text{m}_{\text{CRP}} = \frac{\chi_{\text{C}} \text{m}_{\text{BF}}}{\gamma_{\text{C/CRP}}} \tag{3.24}$$

where m_{BF} is obtained from Equation (3.10), and $\gamma_{\text{C/CRP}}$ is the mass fraction of the carbon in the CRP as follows:

$$\gamma_{C/CRP} = \frac{3}{11} + \frac{12}{77}\gamma_{CO} + \frac{8}{11}\gamma_{soot} \tag{3.25}$$

From the production of the carbon-related products m_{CRP}, the production of soot, carbon monoxide and carbon dioxide can be obtained as follows:

$$\mathrm{m}_{\mathrm{soot}} = \gamma_{\mathrm{soot}} \mathrm{m}_{\mathrm{CRP}} \tag{3.26}$$

$$m_{CO} = \gamma_{CO} m_{CRP} \tag{3.27}$$

$$\mathrm{m}_{\mathrm{CO_2}} = (1 - \gamma_{\mathrm{soot}} - \gamma_{\mathrm{CO}}) \mathrm{m}_{\mathrm{CRP}} \tag{3.28}$$

Water production $\mathrm{m}_{\mathrm{H_2O}}$ and the total unburned fuel m_{TUF} can be obtained as follows:

$$\mathrm{m}_{\mathrm{H_2O}} = 9 \chi_{\mathrm{H}} \mathrm{m}_{\mathrm{BF}} \tag{3.29}$$

$$m_{TUF} = (\chi_C + \chi_H + \chi_O)(m_{PF} - m_{BF}) \tag{3.30}$$

In this model, m_{BF} is assumed to have the same element composition as m_{PF}, and all the hydrogen in the burned fuel is changed into water.

4. FLUID FLOW MODEL

4.1 Plume Entrainment

Fire-induced buoyant plume entrainment is a very important factor in modelling fire growth and smoke spread in a building. A number of formulas can be found in the literature.[39-42] A review of existing models shows that they are based primarily on data from smaller fires.[41, 42]

Some full-scale standard room fire experiments[42] indicated that McCaffrey's model[39] gives the best agreement with the measured entrainment rates, although it does not account for the changing surrounding gas density. In this 2-zone model, McCaffrey's model is used, which has been used by CFAST.

For atria or warehouses, Heskestad's model[43] has been widely used. This correlation is also implemented in the model to have users select either of the two models.

If fires burn along the walls or in corners, plume entrainment rate will be restricted. Mower and Williamson[44] provided modification factors for the normal plume correlation to extend the ability to wall and corner burning geometry as follows:

The mass entrainment rate for centre fires can be expressed as a general function:

$$\dot{m}_e = f(Q_C, Z_e) \tag{4.1}$$

where Q_C is the convection heat release rate, and Z_e is the entrainment height. Then, the mass entrainment rate for wall and corner fires will be:

$$\dot{m}_e = f(\omega Q_C, Z_e)/\omega \tag{4.2}$$

where for a corner fire, ω is 4, for a wall fire, ω is 2, and for a centre fire, ω is 1.

As the entrainment formula is an empirical relation from experiments, its application is limited to the range of the experimental data. To use this equation outside that range, it is necessary to limit the maximum entrainment rate based on energy balance:

$$\dot{m}_e \le \frac{Q_C}{C_P(T_I - T_L)} - \dot{m}_{PF} \tag{4.3}$$

where T_I is assumed to be the interface temperature. Equation (4.3) means that the averaged plume temperature at the interface should be greater than T_I. In this model, T_I is obtained based on Cooper's N percent rule.[45]

4.2 Door/Window Vent Flow

Mass flow through a vertical-vent is driven by the pressure difference between the two sides of the vent, and it can be calculated by integrating Bernoulli's equation along the vertical direction of the vent. However, the flow through a vent may not be unidirectional, i.e., there may be some gas flowing in and some flowing out of the room. In these cases, the integral limit is divided into several parts, each part having the same flow direction. In this model, the integration limits are dealt with in a manner similar to CFAST. For any sub-divided part of a rectangular vent, the formulation used by CFAST to calculate the mass flow rate has been implemented in this model as follows:[3]

$$\dot{m} = \frac{2}{3} C_{DV} A_{DV} \sqrt{2\rho} \left(\frac{P_t + \sqrt{P_t P_b} + P_b}{\sqrt{P_t} + \sqrt{P_b}} \right) \tag{4.4}$$

where P_t and P_b are the pressure differences at the top and bottom position of this part,
ρ is the gas density of source side,
A_{DV} is the area of this part of vent,
C_{DV} is the coefficient of vent flow, which is taken as 0.7 in this model.

When hot smoke flows out of the vent, it may entrain air from the cool lower layer of the neighbouring room and transport it into the upper layer. Similarly, when cool gas enters the hot layer of the neighbouring zone, it may behave like an inverse plume, and will bring upper layer gas into the lower layer under some conditions. For this phenomenon, a method similar to CFAST has been used.[3]

4.3 Ceiling Vent Flow

It is not appropriate to directly use Bernoulli's equation for smoke flow through a ceiling vent, because in addition to pressure difference, buoyant force has to be considered, which may lead to bi-directional exchange flow. Cooper[46-48] gives a model for unstable flow through shallow, horizontal and circular vents under high-Grashof-number conditions, which is the case encountered in a building fire.

In this model, the first step is to compute the Grashof number to judge whether Cooper's model can be used. If the condition is satisfied, then judge whether the flow is under the condition of flooding by comparing the pressure difference of the top and bottom sides with the critical flooding pressure difference.

If the pressure difference is over the flooding value, then unidirectional flow is expected, otherwise, bi-directional exchange flow will exist. The relevant flow rates can be obtained using equations provided in Cooper's model.[46]

In this model, if the condition using Cooper's model is not satisfied, then the volume flow rate is obtained directly using the following uni-directional Bernoulli's equation:

$$\dot{V} = C_{CV} A_{CV} \sqrt{\frac{2\Delta P}{\rho}} \tag{4.5}$$

where C_{CV} is the coefficient of ceiling vent flow, which is taken as 0.61 in this model. A_{CV} is the area of the ceiling vent.

4.4 Mechanical Ventilation

As shown in Figure 1, a specification-type mechanical ventilation model with its opening parallel with ceiling or floor is implemented. Through the opening, smoke can be extracted out of the room to ambient, or ambient air can be supplied into the room. In this model, two parameters can be specified. One is the Z_{ext}, the vertical extension of the opening away from the ceiling surface, another is the mechanical mass ventilation rate $\dot{m}_{Fan}$ or volume ventilation rate $\dot{V}_{Fan}$.

In the case shown in Figure 1, initially, the smoke interface is above the opening elevation, and the exhausted gas is lower layer air only. If the plume entrainment rate at the elevation of the exhaust opening is greater than the exhaust rate, then the interface will be formed under the opening and, after that time, the exhausted gas will be smoke only. If the plume entrainment rate at the elevation of the exhaust opening is less than the exhaust rate, and the smoke exhaust system is assumed to be ideally effective, then the interface will be formed at the opening elevation, and the exhausted gas is assumed to be composed of two parts, smoke and lower layer gas. For this case, the following formulation has been used to identify how much gas is extracted from each zone.

For mass flow rate specification:

$$\dot{m}_{MU} = \min(\dot{m}_{Fan}, \dot{m}_{max}) \tag{4.6}$$

$$\dot{m}_{ML} = \dot{m}_{Fan} - \dot{m}_{MU} \tag{4.7}$$

where $\dot{m}_{MU}$ and $\dot{m}_{ML}$ are mass flow rates exhausted from upper layer and lower layer, respectively. $\dot{m}_{max}$ is the maximum smoke exhaust rate from the upper layer.

Similarly, for volume flow rate specification:

$$\dot{V}_{MU} = \min(\dot{V}_{Fan}, \frac{\dot{m}_{max}}{\rho_U}) \tag{4.8}$$

$$\dot{V}_{ML} = \dot{V}_{Fan} - \dot{V}_{MU} \tag{4.9}$$

where $\dot{V}_{MU}$ and $\dot{V}_{ML}$ are volume flow rate exhausted from upper and lower layers.

The above method of limiting the maximum smoke exhaust rate is helpful in ensuring the numerical stability and efficiency, when the exhausted gas is composed of smoke and the lower layer gas. Sometimes $\dot{m}_{max}$ is difficult to calculate. For the situation shown in Figure 1, where a ceiling vent is not provided and the soffit of the door is lower than the opening, $\dot{m}_{max}$ is the plume entrainment rate at the elevation of the opening.

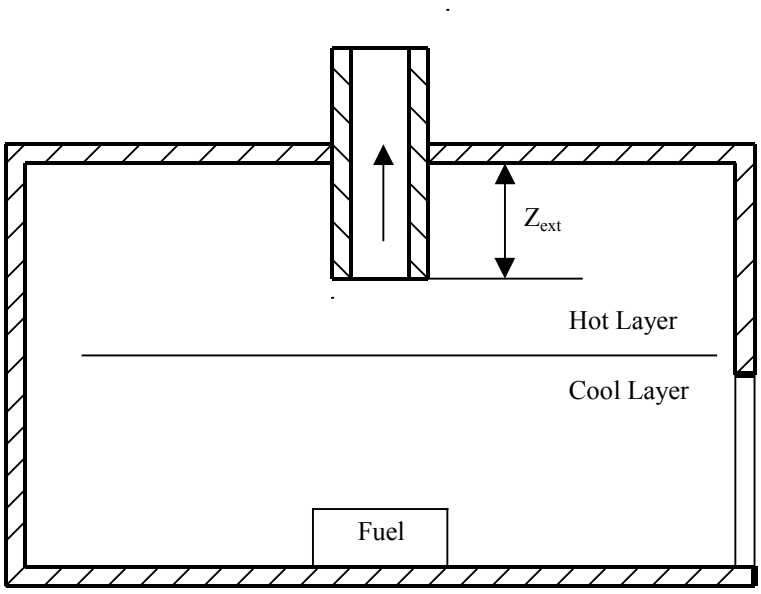

Figure 1. Schematic of the Mechanical Ventilation Opening

4.5 Species Concentration

Suppose at time t, in a well-stirred gas layer, there are NS kinds of species, the total mass is m, and the mass fraction of species K is Y_K, K=1, 2, …, NS.

Then, at the next time step (t+Δt), the concentration of the Kth species will be approximated as follows:

$$(Y_K)_{t+\Delta t} = \frac{mY_K + \Delta t\left[\quad \dot{m}_{e,K} + \quad \dot{m}_{V,K}\right]}{m + \Delta t\left[\quad \dot{m}_e + \quad \dot{m}_V\right]}, \quad \mathrm{K} = 1, 2, \cdots, \mathrm{NS} \tag{4.10}$$

where $\dot{m}_e$ and $\dot{m}_V$ are the total net mass flow rates entering the layer (negative for flowing out) by plume and ventilation. $\dot{m}_{e,K}$ and $\dot{m}_{P,K}$ are the total net mass flow rates of species K entering the layer by plume and ventilation.

In the right side of Equation (4.10), the denominator is the total mass of the layer at (t+Δt). It is composed of two parts, one is the mass m at time t, another one is the mass added to the layer during t to (t+Δt). And the numerator is the total mass of species K at (t+Δt), also composed of two parts, one is the mass at time t, and the other is the mass added to the layer during the time step Δt.

5. HEAT TRANSFER MODEL

5.1 Conduction Heat Transfer

To calculate conduction heat transfer through the compartment boundaries, a one-dimensional and transient conduction model is used. The governing equation is as follows:

$$\frac{\partial \mathrm{T}}{\partial \mathrm{t}} = \frac{\mathrm{K}}{\rho \mathrm{C}} \frac{\partial^2 \mathrm{T}}{\partial \mathrm{x}^2}, \quad 0 \le \mathrm{x} \le \mathrm{L},\ \mathrm{t} \ge 0 \tag{5.1}$$

Due to the complexity of the building geometry, it is assumed that heat is transferred to the outside environment. The following initial and boundary conditions are given:

$$0 \le \mathrm{x} \le \mathrm{L}, \quad \mathrm{t} = 0, \quad \mathrm{T} = \mathrm{T}(\mathrm{x}, 0) \tag{5.2}$$

$$\mathrm{x} = 0, \quad -\mathrm{k}\frac{\partial \mathrm{T}}{\partial \mathrm{x}} = \mathrm{h}_{\mathrm{IC}}(\mathrm{T}_{\mathrm{g}} - \mathrm{T}(0,\ \mathrm{t})) + \mathrm{q}_{\mathrm{IR}} \tag{5.3}$$

$$\mathrm{x} = \mathrm{L}, \quad -\mathrm{k}\frac{\partial \mathrm{T}}{\partial \mathrm{x}} = -\mathrm{h}_{\mathrm{OC}}(\mathrm{T}_{\mathrm{a}} - \mathrm{T}(\mathrm{L},\ \mathrm{t})) - \mathrm{q}_{\mathrm{OR}} \tag{5.4}$$

where T(x, 0) is the temperature profile at the initial time. h_{IC} and h_{OC} are convection heat transfer coefficients of the inside and outside surfaces of a wall, ceiling or floor, and q_{IR} and q_{OR} are the net radiation heat fluxes received by the inside and outside surfaces.

Equations (5.3) and (5.4) as well as the four terms h_{IC}, h_{OC}, q_{IR} and q_{OR} implicate the coupling of conduction with convection and radiation. In this model, the time splitting method is used to couple the heat conduction into the zone model.

The full implicit finite difference method is applied to discretize the equation, and the TDMA (Tri-Diagonal Matrix Algorithm) algorithm is selected to solve the discrete equation.

5.2 Convection Heat Transfer

5.2.1 Convection Heat Transfer in Non-Fire Rooms

Convection heat transfer in a non-fire room may be considered to be a natural convection system. The following equations from CFAST for turbulent convection heat transfer are included in this model:[3, 28, 49, 50]

$$\mathrm{Q_{conv}} = \mathrm{q_{conv}} \mathrm{A_w} \tag{5.5}$$

$$q_{conv} = h(T_g - T_w) \tag{5.6}$$

where Q_{conv} and q_{conv} are convection heat loss and flux to a surface of a wall, ceiling or floor, T_g and T_w are the temperature of gas and the surface, A_w is the area of the surface, and h is the convection heat transfer coefficient.

In Equation (5.6), h is computed using empirical correlations based on Grashof, Prandtl and Nusselt numbers. The detailed formulas can be found in the literature.[3, 28]

5.2.2 Convection Heat Transfer for Ceiling in Fire Rooms

In the fire room, ceiling jet-induced convection heat transfer should be separately evaluated due to its specific magnitude. Heat loss due to a ceiling jet can be calculated using the following formulas:[51-55]

$$Q_{ceil} = \int_A q_{ceil} dA \tag{5.7}$$

$$q_{ceil} = h(T_{ad} - T_{ceil}) \tag{5.8}$$

where Q_{ceil} and q_{ceil} are the gas heat loss and flux to the ceiling surface,
h is the heat transfer coefficient,
T_{ad} and T_{ceil} are characteristic gas and ceiling surface temperatures.

The detailed formulas to calculate h and T_{ad} can be found in the literature.[3, 28, 51-55] In this model, the ceiling surface is converted into an equivalent circular surface with the same surface area, and the plume impingement point is assumed to be at the centre of the surface. The ceiling surface temperature is assumed to be spatially uniform.

5.2.3 Convection Heat Transfer for Wall and Floor in Fire Rooms

In fire rooms, for the lower wall and floor, the convection heat transfer model is the same as in non-fire rooms. For the ceiling surface, the model introduced in the above section is applied to calculate ceiling jet convection heat transfer.

However, for the upper wall of fire rooms, the non-fire room convection model may underestimate the heat transfer due to the wall jet. Thus, in this model, a simple ad hoc treatment is introduced as follows.[6]

The radius of the equivalent circular ceiling surface is denoted as R_C, and the smoke thickness as Z_S.

If $R_C \geq Z_S$, then:

$$q = (Q_{ceil} / A_{ceil} + q_{conv}) / 2 \tag{5.9}$$

If $R_C < Z_S$, then:

$$q = (R_C \times Q_{ceil} / A_{ceil} + Z_S \times q_{conv}) / (R_C + Z_S) \tag{5.10}$$

where q is the convection heat flux of the upper wall,
q_{conv} is the convection heat flux as described in Equation (5.6),
Q_{ceil} and A_{ceil} are the heat loss to the ceiling surface and the ceiling surface area.

5.3 Radiation Heat Transfer

5.3.1 Derivation of Equations

Radiation heat transfer is a very important mechanism in compartment fires, especially in the fire room. A two-surface model is applied in the fire and non-fire rooms, where the ceiling and upper wall are considered to be the upper surface, and the floor and lower wall are considered to be the lower surface. Besides, in the fire room, the flame is assumed to be a sphere with its centre located at the position of half flame height above the fuel bed, and the radiation flux of the sphere to any direction is assumed to be uniform. The sphere is assumed to be the third differential emitting blackbody surface interacting with the upper surface, lower surface and upper layer gas.[6, 20, 29]

The smoke layer is considered to be an absorptive medium, and the lower layer is considered to be transparent. The following radiation heat transfer equation for each surface element k is used:[56]

$$\sum_{j=1}^{N}\left(\frac{\delta_{kj}}{\varepsilon_j}-F_{kj}\frac{1-\varepsilon_j}{\varepsilon_j}\overline{\tau}_{kj}\right)q_j=\sum_{j=1}^{N}\left[\left(\delta_{kj}-F_{kj}\overline{\tau}_{kj}\right)\sigma T_j^4-F_{kj}\overline{\alpha}_{kj}\sigma T_g^4\right] \tag{5.11}$$

where q_j is the net radiation heat transfer rate of surface j,
δ_{kj} is the Kronecker function,
ε_j is the emissivity of surface j,
F_{kj} is the view factor from surface k to surface j,
$\overline{\tau}_{kj}$, $\overline{\alpha}_{kj}$ are geometrical mean transmittance and absorptance from surfaces k to j,
T_j, T_g are the temperatures of surface j and gas.

Thus, for each surface, the following relations can be obtained:

$$k=1,\qquad \left(\frac{1}{\varepsilon_1}-F_{11}\frac{1-\varepsilon_1}{\varepsilon_1}\overline{\tau}_{11}\right)q_1-F_{12}\frac{1-\varepsilon_2}{\varepsilon_2}\overline{\tau}_{12}q_2= \tag{5.12}$$
$$(1-F_{11}\overline{\tau}_{11})\sigma T_1^4-F_{12}\overline{\tau}_{12}\sigma T_2^4-(F_{11}\overline{\alpha}_{11}+F_{12}\overline{\alpha}_{12}+F_{1F}\overline{\alpha}_{1F})\sigma T_g^4-F_{1F}\overline{\tau}_{1F}\sigma T_F^4$$

$$k=2,\qquad -F_{21}\frac{1-\varepsilon_1}{\varepsilon_1}\overline{\tau}_{21}q_1+\left(\frac{1}{\varepsilon_2}-F_{22}\frac{1-\varepsilon_2}{\varepsilon_2}\overline{\tau}_{22}\right)q_2= \tag{5.13}$$
$$-F_{21}\overline{\tau}_{21}\sigma T_1^4+(1-F_{22}\overline{\tau}_{22})\sigma T_2^4-(F_{21}\overline{\alpha}_{21}+F_{22}\overline{\alpha}_{22}+F_{2F}\overline{\alpha}_{2F})\sigma T_g^4-F_{2F}\overline{\tau}_{2F}\sigma T_F^4$$

where subscripts 1, 2, g and F refer to the upper surface, lower surface, smoke layer and flame, respectively. In Equations (5.12) and (5.13), the last term on the right side of each equation is related to the assumed flame radiation. For convenience, the value of the radiation fraction instead of flame temperature is used, and the following relation is applied:

$$F_{1F}\bar{\tau}_{1F}\sigma T_F^4 = Q_F F_{F1}\bar{\tau}_{1F} / A_1 \tag{5.14}$$

$$F_{2F}\bar{\tau}_{2F}\sigma T_F^4 = Q_F F_{F2}\bar{\tau}_{2F} / A_2 \tag{5.15}$$

where Q_F is the radiation heat release rate of the flame, which is a fraction of the total heat release rate of the fire; and A_1 and A_2 are the areas of the upper and lower surfaces.

Substituting Equations (5.14) and (5.15) into (5.12) and (5.13), using the relations of transmittance and absorptance,

$$\bar{\tau}_{ij} = \bar{\tau}_{ji}, \quad \bar{\alpha}_{ij} = \bar{\alpha}_{ji}, \quad \bar{\alpha}_{ij} + \bar{\tau}_{ij} = 1 \tag{5.16}$$

and assuming:

$$\bar{\alpha}_{11} = \bar{\alpha}_{12} = \bar{\alpha}_{F1} = \varepsilon_g \quad \text{and} \quad \bar{\alpha}_{F2} = 0 \tag{5.17}$$

the following formulas for calculating radiation heat transfer can be derived:

$$\begin{cases} q_1 = \dfrac{W_1 \varepsilon_1}{Z} \\ q_2 = \dfrac{W_2 \varepsilon_2}{Z} \end{cases} \tag{5.18}$$

$$\begin{aligned} Z = {} & F_{21}F_{12}(1-\varepsilon_g)^2(1-\varepsilon_1)(1-\varepsilon_2) \\ & -[1-F_{11}(1-\varepsilon_g)(1-\varepsilon_1)][1-F_{22}(1-\varepsilon_2)] \end{aligned} \tag{5.19}$$

$$\begin{aligned} W_1 = {} & \{[1-(1-\varepsilon_g)F_{11}][1-(1-\varepsilon_2)F_{22}]-[(1-\varepsilon_2)(1-\varepsilon_g)^2F_{12}F_{21}]\}\sigma T_1^4 \\ & -(1-\varepsilon_g)F_{12}\varepsilon_2\sigma T_2^4 \\ & -\{1+(1-\varepsilon_2)[(1-\varepsilon_g)F_{12}F_{21}-F_{22}]\}\varepsilon_g\sigma T_g^4 \\ & -\frac{Q_F}{A_1}(1-\varepsilon_g)[F_{21}-\varepsilon_2(F_{F2}-F_{22})] \end{aligned} \tag{5.20}$$

$$\begin{aligned} W_2 = {} & \{[1-(1-\varepsilon_1)(1-\varepsilon_g)F_{11}](1-F_{22})-(1-\varepsilon_1)(1-\varepsilon_g)^2F_{12}F_{21}]\}\sigma T_2^4 \\ & -(1-\varepsilon_g)F_{21}\varepsilon_1\sigma T_1^4 \\ & -\{[1-(1-\varepsilon_1)(1-\varepsilon_g)F_{11}]+(1-\varepsilon_1)(1-\varepsilon_g)\}F_{21}\varepsilon_g T_g^4 \\ & -\frac{Q_F}{A_2}\{F_{F2}+(1-\varepsilon_1)(1-\varepsilon_g)[F_{F1}F_{12}(1-\varepsilon_g)-F_{F2}F_{11}]\} \end{aligned} \tag{5.21}$$

$$Q_g = -(A_1 q_1 + A_2 q_2) + Q_F \tag{5.22}$$

where Q_g is the radiation heat gain rate of the smoke layer.

Equations (5.18) to (5.22) are applicable to both fire and non-fire rooms. For fire rooms, the radiation heat release rate Q_F is not zero, while for non-fire rooms, Q_F is zero.

To couple the two-surface radiation model with the four-surface convection and conduction models, the following approach is used. The upper surface temperature in the radiation model employs the higher temperature of the ceiling surface and upper wall surface used in the convection and conduction models. Similarly, the lower surface temperature in the radiation model employs the higher temperature of the floor surface and the lower wall surface used in the conduction and convection models.

5.3.2 Calculation of View Factors

It is simple to get the values of F_{11}, F_{12}, F_{21} and F_{22} as follows:

$$F_{12} = A_{\text{int}} / A_1, \quad F_{11} = 1 - F_{12} \tag{5.23}$$

$$F_{21} = A_{\text{int}} / A_2, \; F_{22} = 1 - F_{21} \tag{5.24}$$

As mentioned above, the flame is assumed to be a black sphere radiating uniformly. Shown in Figure 2, Point F is assumed to be the centre of the sphere from which heat is radiated uniformly. The view factor from F to area A (OBCD) is obtained:

$$\xi = \int_A \frac{\cos\theta}{4\pi (FK)^2} dA \tag{5.25}$$

Integrating the above equation, gives:

$$\xi = \frac{1}{4\pi} \arcsin\left[\frac{1}{\sqrt{(x^2+1)(y^2+1)}} \right] \tag{5.26}$$

$$where\ x = \frac{OF}{OB}, \quad y = \frac{OF}{OD}$$

The view factors F_{F1} and F_{F2} in Equations (5.20) and (5.21) can be obtained from Equation (5.26).

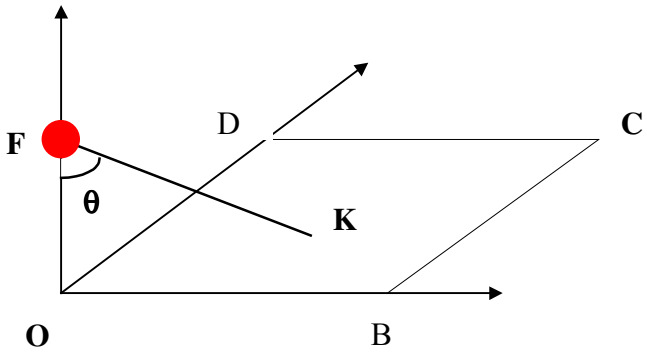

Figure 2. Schematic of Flame Radiation to a Rectangular Surface

5.3.3 Gas Emissivity

Gas emissivity for carbon dioxide, water vapour and soot can be obtained as follows:[56, 57]

$$\varepsilon = \varepsilon_{soot} + \varepsilon_g - \varepsilon_{soot}\varepsilon_g \tag{5.27}$$

$$\varepsilon_g = \varepsilon_{CO_2} + \varepsilon_{H_2O} - \varepsilon_D \tag{5.28}$$

$$\varepsilon_{soot} = 1 - \frac{1}{(1 + 350 C_{soot} Le T_g)^4} \tag{5.29}$$

where C_{soot} is the volume fraction of soot in the smoke layer,
Le is the equivalent mean beam length of the smoke layer,
ε_D is emittance reduction resulting from spectral overlap.

$$\varepsilon_{CO_2} = 6.17\sqrt{T_g}(P_{CO_2} Le)^{1/3} \tag{5.30}$$

$$\varepsilon_{H_2O} = 0.674[1 - \exp(-1.32\sqrt{\Psi})] \tag{5.31}$$

$$\Psi = P_{H_2O} Le(300/T_g)[P_g + (5\sqrt{300/T_g} + 0.5)P_{H_2O}] \tag{5.32}$$

where P_g is the gas pressure,
P_{CO_2} and P_{H_2O} are the partial pressure of CO_2 and H_2O.

$$\varepsilon_D = F(T_g)G(\xi)\{\log[101.3(P_{CO_2} + P_{H_2O})Le]\}^{2.76} \tag{5.33}$$

$$F(T_g) = -1.0204\times10^{-6} T_g^{\,2} + 0.002449 T_g - 0.23469 \tag{5.34}$$

$$G(\xi) = \xi/(10.7 + 101\xi) - \xi^{10.4}/111.7 \tag{5.35}$$

$$\xi = P_{H_2O}/(P_{H_2O} + P_{CO_2}) \tag{5.36}$$

6. NUMERICAL METHOD

6.1 Solution Strategy

There are a number of numerical methods that can be used to solve the governing equations derived in Section 2. One approach, which is also used by CFAST, solves the full system of equations for all compartments simultaneously. Another approach is to solve the equations room by room, i.e., each time only the equations of one room are solved, and the final solution is obtained by iteration. A third approach is to solve the system of equations group by group, i.e., each time only the equations of a group of rooms having similar physical or numerical characteristics are solved, and the final solution is obtained by iteration.

The simultaneous solution method is the easiest to implement using existing ODE solvers. This method was initially used in this model, however, for cases with a large number of compartments, it was not converging well. The method currently used in the model is the room by room iterative method. With this method, it is easier to identify the sources of convergence problems and easier for ODE solvers to converge. In addition, with this method, different algorithms can be used for different compartments. In this model, two algorithms have been implemented; one is an ODE solver for the compartments with smoke or fire, and another one is an algebraic equation solver for the compartments without smoke or fire.

The solution procedure is as follows. As shown in Figure 3, for each compartment, if the compartment has smoke or fire, then the LSODA[30] solver is used to integrate the ODEs from t to (t+Δt); and if the compartment has no temperature rise, then the Steffensen Acceleration Method[31] is used to solve the non-linear algebraic equation. After sweeping through all the compartments the process is repeated until convergence is achieved.

Also as shown in Figure 3, for each step of the ODE solver, the mass and energy source terms of the governing equation set are computed using the equations given in Sections 3, 4 and 5. For each step of the Steffensen Acceleration Method, the flow rate of each vent connected to the compartment being solved is also computed using the related equations given in Section 4.

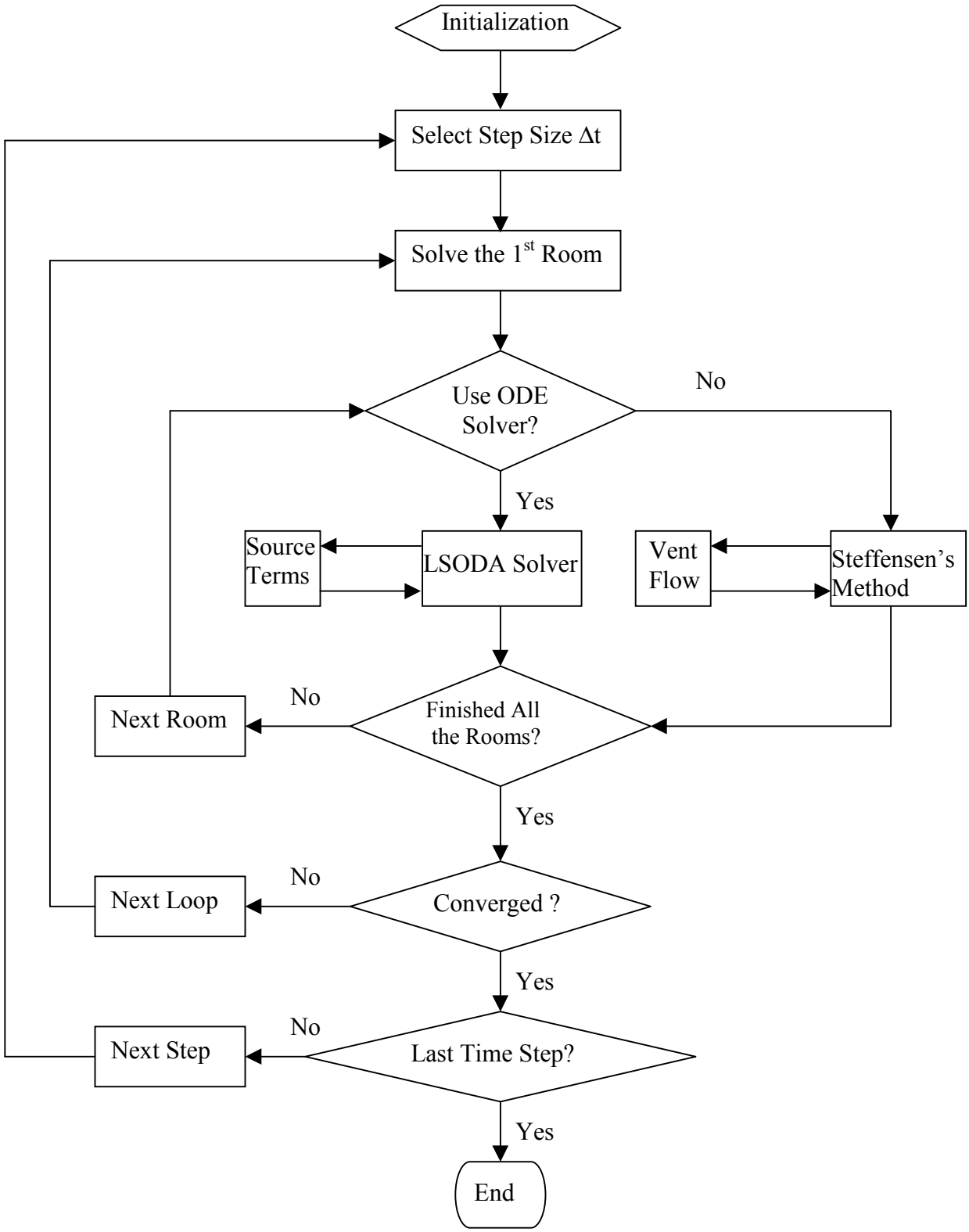

Figure 3. Flow Chart of the Numerical Calculation

6.2 Numerical Properties of the ODE System

There are many ways to select the four independent governing ODEs for each compartment with fire or smoke. As mentioned in Section 2, the form of the equations implemented in the model is composed of the following four variables: pressure, upper layer enthalpy, upper layer mass and lower layer mass. As analyzed by Forney[33] for the equation of mass, this formulation does not have the vanishing denominator problem of the density or temperature equation. However, quantities derived from enthalpy and mass such as density are only valid when a layer volume has a significant number of accurate digits.

One significant property of the equation set is the presence of multiple time scales.[3, 58] For example, combustion chemical reaction has the fastest time scale. In this model, this scale is avoided by assuming infinitely fast chemical reaction. Parameters related to fluid flow have a much slower scale than chemical reaction but a much faster scale than conduction. In mathematics, this property is known as stiffness, which means the equation set has a very large ratio of the maximum eigenvalue to its minimum eigenvalue of the related Jacobian matrix.

Stiffness property will affect the numerical calculation of the equation set.[59] In fact, to maintain numerical stability, if non-stiff methods such as those of Runge-Kutta or Adams are applied to solve the equation set, the choice of the step size will be dominated by stability, not accuracy. This property requires the application of special numerical solution methods.[59] Backward differentiation formulas (BDFs) are generally used to solve the stiff problems.[60]

There are a number of ODE solvers available to solve the stiff ODE system.[60] In this model, an ODE solver called LSODA,[30] is used to integrate the equation set numerically. LSODA is a descendant of DIFSUB,[59] a pioneering stiff ODE solver, developed by Gear using the BDF method.

Due to its implicitness, an iteration process composed of prediction and correction is applied. The Newton iteration method is used to obtain the solution. The order and step size are automatically chosen by the solver through estimating the local truncation error.

Both the model and its interface are coded using MS Visual Basic Version 5. Thus, the ODE solver LSODA was converted to Visual Basic from FORTRAN.

More details can be found in the literature.[28]

7. VALIDATION EXAMPLES

In this section, two examples of model predictions are compared to two sets of experimental data from the literature.[45, 61]

7.1 Single Compartment Example

Dembsey et al[61] reported results on twenty compartment fire experiments suitable for model comparison in a single compartment (2.5 m × 3.7 m in plan and 2.5 m in height) that is similar in size, geometry and construction to the standard fire test compartment. The compartment has a single doorway, 0.76 m wide × 2.0 m high, centered on one of the shorter sides. A 0.61 m × 1.22 m porous surface burner was placed into the compartment with its porous surface being 0.61 m above the floor. The propane-fired burner supplied heat at a steady rate between 330 and 980 kW for the duration of each experiment. Furthermore, three sets of experimental data with heat release rates (HRR) at 330 kW, 630 kW and 980 kW were compared to two comprehensive compartment fire models, CFAST and FIRST.

In this study, the model predictions are compared to the experimental data of the reference 61. The input and output data of the model are shown in Table 1 and Table 2, respectively. In Table 2, for each HRR, there are four rows to describe the experimental data, CFAST's prediction, FIRST's prediction and the prediction of this model, respectively. The fire duration time of each experiment is provided, which is taken as the fire simulation time of the model. The fire end time is the point at which the model predictions are compared to the experimental data. The used CPU time of each case using a Pentium 450 PC is also presented in the table.

Table 1. Zone Model Input Data For Single Compartment Example

Fuel Properties			
Fuel	Propane (C_3H_8)	χ_H	0.18
Heat of Combustion (MJ/kg)	44	χ_C	0.82
Radiation Fraction[61, 62]	0.27	γ_{soot}	0
Nominal HRR (kW)	330, 630, 980	γ_{co}	0
Ambient Conditions			
Pressure (Pa)	101300	Temperature (°C)	20
Thermal Properties of Compartment Boundaries			
	Ceiling	Wall	Floor
Thickness (m)	0.066	0.054	0.044
Density (kgm^{-3})	449	449	770
Conductivity ($Wm^{-1}K^{-1}$)	0.10	0.10	0.14
Specific heat ($Jkg^{-1}K^{-1}$)	1090	1090	900
Surface Emissivity	0.9	0.9	0.9
Dimensions			
	Depth (m)	Width (m)	Height (m)
Compartment	2.5	3.7	2.5
Vent	N/A	0.76	2.0
Burner's surface location	1.25	1.85	0.61

Table 2. Comparison of Models' Prediction with Experimental Data

Parameters	T_U	T_L	T_{WU}	T_{WL}	T_{FLR}	Z_I	Z_N	ΔP_F	$\dot{m}_{AV}$	q_{IF}
Units	°C	°C	°C	°C	°C	m	m	Pa	kg/s	kW/m^2
HRR=330 (kW), Duration Time=30 (min) , Run Time=3 s										
Experimental	370	84	315	187	180	1.12	1.04	-1.97	0.87	3.8
CFAST	457	48	426	372	334	1.31	1.08	-1.11	0.64	16
FIRST	278	26	245	N/A	N/A	1.15	N/A	N/A	0.67	N/A
FIERA	408	80	359	337	249	1.29	0.98	-1.88	0.73	11
HRR=630 (kW), Duration Time = 35 (min) , Run Time=5 s										
Experimental	610	179	566	342	377	1.04	0.94	-3.88	1.03	13
CFAST	730	88	711	672	655	1.18	0.96	-2.13	0.78	57
FIRST	476	36	376	N/A	N/A	1.10	N/A	N/A	0.71	N/A
FIERA	585	104	585	545	391	1.06	0.97	-2.44	0.83	31
HRR=980 (kW), Duration Time=20 (min), Run Time=6 s										
Experimental	796	236	728	471	551	0.99	0.92	-4.36	1.01	33
CFAST	901	118	885	852	841	0.96	0.95	-2.82	0.89	107
FIRST	642	61	483	N/A	N/A	1.09	N/A	N/A	0.74	N/A
FIERA	785	122	785	754	531	0.89	0.93	-2.87	0.89	71

T_U , T_L : upper, lower layer temperatures; T_{WU} , T_{WL} : upper, lower wall interior surface temperatures; T_{FLR} : interior surface temperature of floor; Z_I , Z_N : interface, neutral plane heights; ΔP_F : floor pressure difference to ambient; $\dot{m}_{AV}$: average vent mass flow rate; q_{IF} : floor radiant incident heat flux.

7.2 Two-Compartment Example

Cooper et al[45] reported a series of multi-compartment fire experiments. In this study, a set of that experimental data is compared to the model prediction. The test space involved two compartments, a burn room and a corridor. The heat release rate was a linearly growing fire with the relation: Q=C t, C=30 kW/min. There was a 2.0 m high and 1.07 m wide door between the burn room and the corridor. Additionally, a 0.15 m × 0.94 m hole to the ambient space was provided in a wall of the corridor. The model input data is shown in Table 3. Figures 4 to 6 present the comparisons for averaged gas temperature rise, interface height and pressure difference between the two compartments near the ceiling. The used CPU time for this case using the Pentium 450 PC is 25 seconds, the step size Δt is 2 seconds, and the number of iteration times is one.

Table 3. Zone Model Input Data For Two-Compartment Example

Fuel Properties			
Fuel	Methane (CH_4)	χ_H	0.25
Heat of Combustion (MJ/kg)	50.0	χ_C	0.75
Radiation Fraction[63]	0.24	γ_{soot}	0
Nominal HRR (kW)	30t (t: min.)	γ_{co}	0
Ambient Conditions			
Pressure (Pa)	101300	Temperature (°C)	25
Thermal Properties of Compartment Boundaries			
	Ceiling	Wall	Floor
Thickness (m)	0.013	0.013	1.0
Density (kgm^{-3})	790	790	1950
Conductivity ($Wm^{-1}K^{-1}$)	0.2	0.2	0.8
Specific heat ($Jkg^{-1}K^{-1}$)	900	900	860
Emissivity	0.9	0.9	0.9
Dimensions			
	Depth (m)	Width (m)	Height (m)
Burn room	3.3	4.3	2.36
Corridor	2.4	11.1	2.36
Vent from burn room to corridor	N/A	1.07	2.0
Vent from corridor to ambient	N/A	0.94	0.15
Burner's surface location	1.65	2.15	0.24

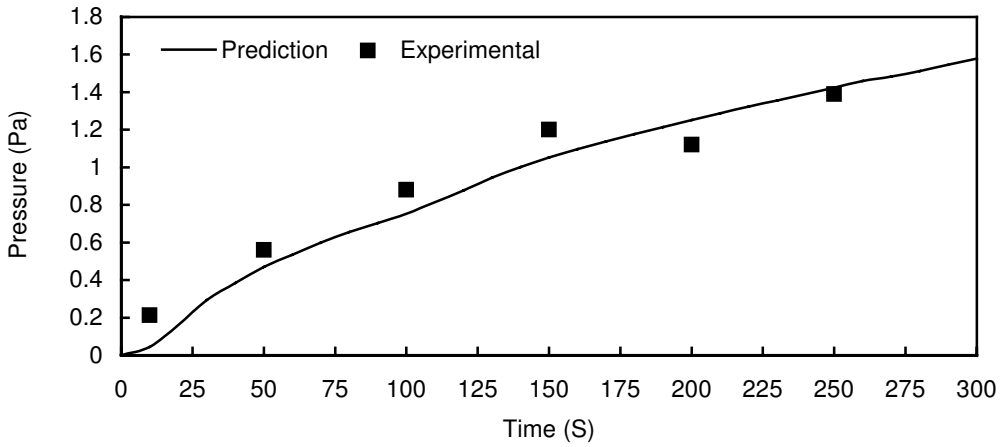

Figure 4. Pressure Difference Between the Burn Room and Corridor Near the Ceiling

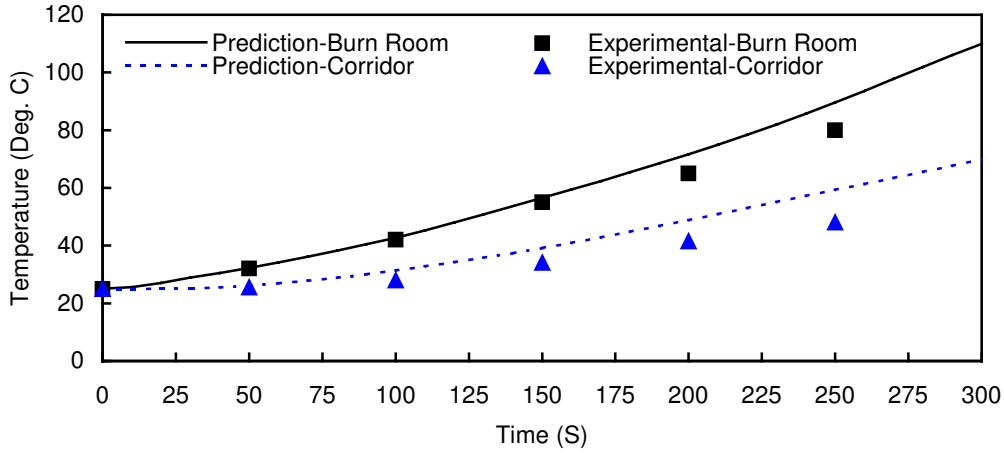

Figure 5. Averaged Gas Temperatures of the Burn Room and Corridor

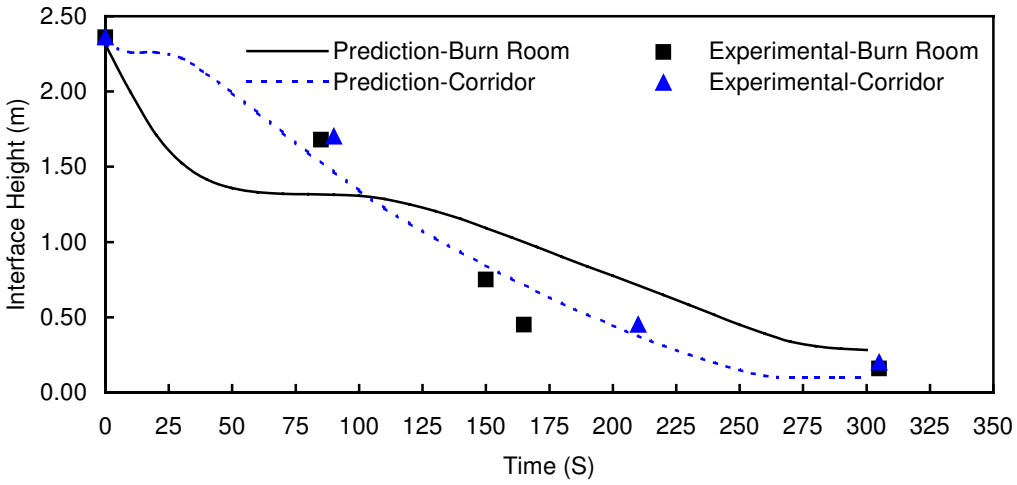

Figure 6. Interface Heights of the Burn Room and Corridor

7.3 Analysis of the Simulation Results

For the case of the single compartment, it is shown that this model gives favourable results for the parameters compared, especially for upper layer temperature, interface height, neutral plane height and vent flow rates.

However, the model overestimates the floor incident radiation heat flux and the lower wall surface temperature. This may be due to the two-surface radiation heat transfer model. This may also be affected by the value of the radiation fraction.

Furthermore, the lower layer gas temperature is obviously underestimated, especially when the HRR is raised. As already described, in this model, two factors affect the lower layer temperature. One is the convection heat transfer from the lower wall and floor, the other is the inverse cold plume entrainment when outside cold air enters the lower layer through the upper layer. However, in real fires, there are other mechanisms affecting the lower layer temperatures, such as mass mixing between the upper and lower layers and radiation absorption of the contaminated lower layer, which has not been accounted for in this model.

For the case of two compartments, Figures 4 to 6 show that the model also gives favorable results when compared to the experimental data.

8. CONCLUSION

In this model, 2-zone ODE equations are solved only for compartments with fire or smoke; for other compartments, non-linear algebraic equations are solved. The enthalpy of the upper layer is selected as the solution variable of the ODEs, and it is working well.

A room by room iteration method has been developed to solve the governing equations. The LSODA ODE solver has been modified and used to solve the ODEs for rooms with fire or smoke, and the Steffensen Acceleration Method is used to solve the algebraic equations for rooms without fire or smoke.

Experimental data for single and two compartment tests are compared to the prediction of the model. For both cases, favourable results have been obtained.

ACKNOWLEDGMENT

The authors would like to thank the Canadian Department of National Defence for contributing to the funding of the project, as well as the Natural Sciences and Engineering Research Council of Canada (NSERC) for offering the opportunity to Dr. Zhuman Fu to conduct post-doctorate research work at the National Research Council of Canada through the NSERC Visiting Fellowship program.

REFERENCES

1. Jones, W.W. & Forney, G.P., Improvement in predicting smoke movement in compartmented structures. Fire Safety Journal, 21 (1993) 269.
2. Jones, W.W., A multi-compartment model for the spread of fire, smoke and toxic gases. Fire Safety Journal, 9 (1985) 55.

3. Peacock, R.D., Forney, G.P., Reneke, P., Portier, R. & Jones, W.W., CFAST, The consolidated model of the fire growth and smoke transport. NIST Technical Note 1299, Gaithersburg, MD, 1993.
4. Jones, W.W. & Peacock, R.D., Refinement and experimental verification of a model for fire growth and smoke transport. Second International Symposium on Fire Safety Science, 1988.
5. Quintiere, J.G., Compartment fire modelling. The SFPE Handbook of Fire Protection Engineering, Quincy, MA: National Fire Protection Association, 1995, p.3-125.
6. Fu, Z. & Fan, W., A zone-type model for a building fire and its sensitivity analysis. Fire and Materials, 20 (1996) 215.
7. Friedman, R., An international survey of computer models for fire and smoke. Journal of Fire Protection Engineering, 4 (1992) 81.
8. Jones, W.W., The evolution of hazard, the fire hazard assessment methodology. Fire Technology, 2nd Quarter, 1997, p. 167.
9. Walton, W.D., Zone computer fire models for enclosures. The SFPE Handbook of Fire Protection Engineering, Quincy, MA: National Fire Protection Association, 1995, p. 3-148.
10. Kawagoe, K., Fire behavior in rooms. Building Research Institute, Ministry of Construction (Japan), Report No. 27, Tokyo, 1958.
11. Cox, G., Compartment fire modelling, Chapter 6 of " Combustion Fundamentals of Fire", edited by Cox, G., Academic Press, 1995.
12. Thomas, P.H., Hinkley, P.L., Theobald, C.R. & Simms, D.L., Investigations into the flow of hot gases in roof venting. Fire Research Technical Paper No.7, HMSO, London, 1963.
13. Janssens, M., Room fire models, Chapter 6 of "Heat Release in Fires", edited by Babrauskas, V. & Grayson, S.J., Elsevier Applied Science, 1992.
14. Peacock, R.D., Davis, S. & Babrauskas, V., Data for room fire model comparisons. Journal of Research of the NIST, 96 (1991) 411.
15. Fowkes, N.D., "A mechanistic model of the 1973 and 1974 bedroom test fires" in Croce, P.A., ed., "A study of room fire development: The second full-scale bedroom fire test of the home fire project (July 24, 1974)", Vol. II, FMRC Tech. Report No. 21011.4, 1975, pp. 8-50.
16. Quintiere, J.G., "Growth of fire in building compartments" in Robertson, A.F., ed., Fire Standards and Safety, ASTM STP614, American Soc. For Testing and Materials, 1977, pp. 131-167.
17. Pape, R. & Waterman, T., Modification to the FIRES pre-flashover room fire computer model, IITRI Project J6400, IIT Res. Inst., Chicago, 1977.
18. Mitler, H.E., The physical basis for the Harvard computer fire code. Home Fire Project Report 34, Harvard University, 1978.
19. Barnett, J.R., The WPI/Fire room fire computer model. Proceedings of the 1st Asian Conference on Fire Science and Technology, Hefei, China, 1992, P. 313.
20. Tanaka, T., A model of multi-room fire spread. IR 83-2718, National Bureau of Standards, Washington, DC, 1983.
21. Mitler, H.E. & Rockett, J.A., Users' guide to FIRST, a comprehensive single-room fire model. NBSIR 87-3595, NBS, Gaithersburg, MD, 1987.

22. Jones, W.W. & Peacock, R.D., Technical reference guide for FAST version 1.8. NIST Technical Note 1262, Gaithersburg, MD, 1989.
23. Cooper, L.Y. & Forney, G.P., The consolidated compartment fire model (CCFM) computer code application CCFM.VENTS, Parts 1, 2, 3 and 4. NIST, Gaithersburg, MD, 1990.
24. Yung, D., Hadjisophocleous, G.V., Proulx, G. & Kyle, B.R., Cost effective fire safety upgrade options for a Canadian government office building. Proceedings of the International Conference on Performance Based Codes and Fire Safety Design Methods, Ottawa, ON, 1996.
25. Hadjisophocleous, G.V. & Yung, D., A model for calculating the probabilities of smoke hazard from fires in multi-story buildings. Journal of Fire Protection Engineering, 4 (1992) 67.
26. Takeda, H. & Yung, D., Simplified fire growth models for risk-cost assessment in apartment buildings. Journal of Fire Protection Engineering, 4 (1992) 53.
27. Hadjisophocleous, G.V. & Torvi, D.A., Development of a fire risk assessment computer model for light industrial buildings. Canadian Society of Mechanical Engineering (CSME) Forum, Ryerson Polytechnic University, Toronto, ON, Volume 3, 1998, p. 305.
28. Fu, Z. & Hadjisophocleous, G., Smoke movement model, FIERAsystem Theory Report, IRC-IR-795, National Research Council of Canada, Ottawa, ON, 1999.
29. Fu, Z. & Fan, W., Calculation of the radiation heat transfer in a zone model for building fires. Journal of China University of Science and Technology, 26 (1996) 375. (in Chinese)
30. Petzold, L., Automatic selection of methods for solving stiff and nonstiff systems of ordinary differential equations. SIAM J. SCI. STAT. COMPUT., 4 (1983) 136.
31. Mathews, J.H., Numerical Methods for Mathematics, Science, and Engineering, Prentice Hall, Englewood Cliffs, NJ, 1992.
32. Wylen, G.J.V. & Sonntag, R.E., Fundamentals of Classical Thermodynamics, 2nd edition, John Wiley & Sons, 1978.
33. Forney, G.P., Analyzing and exploiting numerical characteristics of zone fire models. Fire Science and Technology, 14 (1994) 49.
34. Walton, G. N., CONTAM96 user manual. NISTIR 6056, Gaithersburg, MD, 1997.
35. Huggett, C., Estimation of the rate of heat release by means of oxygen consumption. Journal of Fire and Flammability, 12 (1980).
36. Parker, W.J., Calculation of the heat release rate by oxygen consumption for various applications. Journal of Fire Sciences, 2 (1984) 380.
37. Standard Test Method for Heat and Visible Smoke Release for Materials and Products Using Oxygen Consumption Calorimeter, ASTM E1354-90, ASTM, Philadelphia, PA, 1990.
38. Morehart, J.H., Zukowski, E.E. & Kubota, T., Characteristics of large diffusion flames in a vitiated atmosphere. 3rd International Symposium on Fire Safety Science, Edinburgh, 1991.
39. McCaffrey, B.J., Momentum implications for buoyant diffusion flames. Combustion and Flame, 52 (1983) 149.
40. Cetegen, B.M., Zukoski, E.E. & Kubota, T., Entrainment in the near and far field of fire plumes. Combustion Science and Technology, 39 (1984) 305.

41. Zukoski, E.E., Mass flux in fire plumes. Proceedings of the Fourth International Symposium on Fire Safety Science, International Association for Fire Safety Science, 1994.
42. Dembsey, N.A., Pagni, P.J. & Williamson, R.B., Compartment near-field entrainment measurements. Fire Safety Journal, 24 (1995) 383.
43. Heskestad, G., Fire plumes. The SFPE Handbook of Fire Protection Engineering, Quincy, MA: National Fire Protection Association, 1995, p. 2-9.
44. Mowrer, F. W. & Williamson R. B., Estimating room temperatures from fires along walls and in corners. Fire Technology, 23 (1987) 133.
45. Cooper, L.Y., Harkleroad, M., Quintiere, J.G. & Rinkinen, W.J., An experimental study of upper hot layer stratification in full-scale multi-room fire scenarios. Journal of Heat Transfer, 104 (1982) 741.
46. Cooper, L.Y., Combined buoyancy and pressure-driven flow through a shallow, horizontal, circular vent. Journal of Heat Transfer, 117 (1995) 659.
47. Cooper, L.Y., VENTCF2: an algorithm and associated FORTRAN 77 subroutine for calculating flow through a horizontal ceiling/floor vent in a zone-type compartment fire model. Fire Safety Journal, 28 (1997) 253.
48. Cooper, L.Y., Calculating combined buoyancy- and pressure-driven flow through a horizontal, circular vent - Application to a problem of steady burning in a ceiling-vented enclosure. Fire Safety Journal, 27 (1996) 23.
49. Kreith, F., Principles of Heat Transfer, 3rd edition, Intext Educational Publishers, New York, NY, 1976.
50. Holman, J.P., Heat Transfer, McGraw-Hill, 1986, p. 323
51. Cooper, L.Y., Heat transfer from a buoyant plume to an unconfined ceiling. Journal of Heat Transfer, 104 (1982) 446.
52. Cooper, L.Y., The buoyant plume-driven adiabatic ceiling temperature revisited. Journal of Heat Transfer, 108 (1986) 822.
53. Cooper, L.Y., Heat transfer in compartment fires near regions of ceiling-jet impingement on a wall. Journal of Heat Transfer, 111 (1990) 455.
54. Cooper, L.Y., Fire-plume-generated ceiling jet characteristics and convective heat transfer to ceiling and wall surfaces in a two-layer zone-type fire environment. NISTIR 4705, Gaithersburg, MD, 1991.
55. Motevalli, Y. & Ricciuti, C., Characterization of the confined ceiling jet in the presence of an upper layer in transient and steady-state conditions. NIST-GCR-92-613, Gaithersburg, MD, 1992.
56. Siegel, R. & Howell, J., Thermal Radiation Heat Transfer, 2nd edition, Hemisphere Publishing Corporation, 1981.
57. Dietenberger, M.A., Technical reference and user's guide for FAST/FFM version 3, NIST-GCR-91-589, Gaithersburg, MD, 1991.
58. Rehm, R.G. & Forney, G.P., A note on the pressure equations used in zone fire modelling. NISTIR-4906, Gaithersburg, MD, 1992.
59. Gear, C.W., Numerical Initial Value Problems in Ordinary Differential Equations, Prentice Hall, Englewood Cliffs, NJ, 1971.
60. Shampine, L.F., Numerical Solution of Ordinary Differential Equations, Chapman & Hall, New York, NY, 1994.

61. Dembsey, N.A., Pagni, P.J. & Williamson, R.B., Compartment fire experiments: comparison with models. Fire Safety Journal, 25 (1995) 187.
62. Tewarson, A., Generation of heat and chemical compounds in fires. In the SFPE Handbook of Fire Protection Engineering, Quincy, MA: National Fire Protection Association, 1995, p. 3-53.
63. McCaffrey, B., Measurements of the radiative power output of some buoyant diffusion flames, Western States Section, Combustion Institute, WSS/CI 81-15, Pullman, WA, 1981.